

# SEMI-UFORMER: SEMI-SUPERVISED UNCERTAINTY-AWARE TRANSFORMER FOR IMAGE DEHAZING

Ming Tong<sup>1</sup>, Yongzhen Wang<sup>1</sup>, Peng Cui<sup>2</sup>, Xuefeng Yan<sup>1</sup>, Mingqiang Wei<sup>1</sup>

<sup>1</sup>Nanjing University of Aeronautics and Astronautics

<sup>2</sup>PLA Dalian Naval Academy

## ABSTRACT

Image dehazing is fundamental yet not well-solved in computer vision. Most cutting-edge models are trained in synthetic data, leading to the poor performance on real-world hazy scenarios. Besides, they commonly give deterministic dehazed images while neglecting to mine their uncertainty. To bridge the domain gap and enhance the dehazing performance, we propose a novel semi-supervised uncertainty-aware transformer network, called Semi-UFormer. Semi-UFormer can well leverage both the real-world hazy images and their uncertainty guidance information. Specifically, Semi-UFormer builds itself on the knowledge distillation framework. Such teacher-student networks effectively absorb real-world haze information for quality dehazing. Furthermore, an uncertainty estimation block is introduced into the model to estimate the pixel uncertainty representations, which is then used as a guidance signal to help the student network produce haze-free images more accurately. Extensive experiments demonstrate that Semi-UFormer generalizes well from synthetic to real-world images.

**Index Terms**— Semi-UFormer, Uncertainty-aware, Semi-supervised, Transformer, Image dehazing

## 1. INTRODUCTION

Images captured in hazy weather often suffer from noticeable visibility degradation, color distortions, and contrast reduction, which further drop the performance of downstream vision-based systems such as object detection, autonomous driving, and traffic surveillance [1, 2]. Therefore, restoring clean images from their hazy versions is quite important.

Existing dehazing efforts can be roughly classified into prior-based [3, 4] and learning-based approaches [5, 6]. Traditional prior-based studies often exploit hand-crafted image priors to solve the image dehazing problem based on the atmospheric scattering model [7], such as dark channel prior (DCP) [3], non-local color prior [4], etc. Although these algorithms can improve the overall visibility of the image, they are not always reliable due to over-reliance on assumptions.

Recent advances in deep learning open up huge opportunities for image dehazing tasks, and a large number of

learning-based approaches have sprung up [5, 6, 8, 9]. While these algorithms are efficient and can produce promising results on various popular benchmarks, most of them are trained on synthetic data, so they cannot generalize well to real-world scenes due to the existence of domain gap. Recently, several semi-supervised [10, 11] and unsupervised [12, 13] methods have attempted to solve the domain shift issue via training models on real-world images. Although these approaches alleviate the domain shift issue to some extent, their dehazing capacity is usually limited because the ground-truth of real-world hazy images cannot be used as the reconstruction loss to constrain the training of the network.

In addition, most learning-based dehazing efforts only produce the final dehazed images without discussing the uncertainty of the results, which is important for recovering edge and texture regions in hazy images. Furthermore, current dehazing models typically treat all pixels equally, but pixels in edge and texture regions obviously contain more visual information than pixels in smooth regions [14], and such pixels tend to have a high degree of uncertainty. Therefore, accurate estimation and appropriate use of image uncertainty can guide the network to focus on pixels with large uncertainty, so that pixels in specific regions can be enhanced to improve the quality of the final dehazed images.

To resolve these issues, we propose a novel semi-supervised uncertainty-aware transformer network (Semi-UFormer) for image dehazing. Semi-UFormer builds itself on the knowledge distillation framework and benefits from uncertainty guidance information, thus producing much clearer images with well-preserved details. In summary, our contributions are three-fold: (1) A novel semi-supervised uncertainty-aware transformer network called Semi-UFormer is proposed for image dehazing, which leverages both real-world data and uncertainty guidance information to boost the model’s dehazing ability. (2) An uncertainty estimation block is exploited to predict the epistemic uncertainty of the dehazed images, which is then used to guide the network to better reconstruct the image texture and edge regions. (3) We leverage knowledge distillation technology to align the feature distributions between synthetic and real data, which can help the network generalize well in real-world scenarios.

## 2. SEMI-UFORMER

Beyond existing image dehazing wisdom, Semi-UFormer fully explores knowledge distillation technology and uncertainty guidance information to help the network produce much clearer images with more confidence. Fig. 1 exhibited the overview of our Semi-UFormer, where the teacher and student network share the same architecture. We first train the teacher network on both synthetic and real-world data to produce the coarse dehazed results and pixel uncertainty map,  $\theta$ . Then, the student network produces fine dehazed results with the help of uncertainty-guided information  $\theta$  and knowledge distillation strategies. The specific dehazing process is described in the following. In the following, we will detail the individual network modules in our Semi-UFormer.

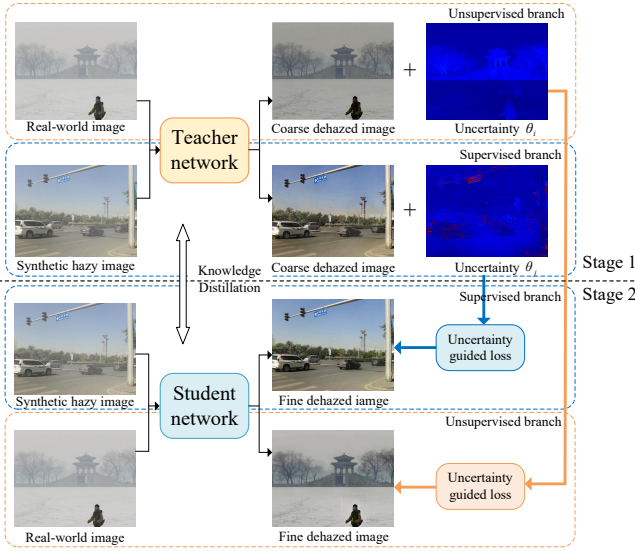


**Fig. 1.** Overall architecture of Semi-supervised Uncertainty-aware Transformer Network (Semi-UFormer).

### 2.1. Teacher-student Network with Knowledge Distillation

Unlike existing image dehazing networks that are exclusively trained on synthetic data, we serve the teacher-student network as the semi-supervised framework and utilize knowledge distillation to migrate supervised dehazing knowledge to unsupervised dehazing.

**Teacher-student network.** The training phase of Semi-UFormer can be divided into two stages, as depicted in Fig. 1. In stage 1, the teacher network is trained on both synthetic and real data to estimate uncertainty information and coarse dehazed images, where the supervised branch plays a leading role. In stage 2, we first leverage the weights of teacher network to initialize the student model. Then, with the help of the teacher network, the student model retrain on both data

and exploits knowledge distillation for better generalization in real-world scenes, where the unsupervised branch plays a leading role. At the same time, the uncertainty  $\theta$  supplied by the teacher model is used as additional guidance information to teach the student how to produce fine dehazed images, while the network for estimating uncertainty  $\theta$  is frozen.

**Knowledge Distillation.** Considering similar images tend to demonstrate correlation at the high-dimensional feature level, we leverage the teacher-student framework to extract the high-dimensional features of synthetic and real haze. Then, we minimize the KL divergence between these two features to reduce the gap between synthetic and real-world data [15], to help the student model apply the supervised dehazing knowledge to unsupervised haze removal.

### 2.2. Transformer-based Dehazing Network

Typically, real-world images follow a definite rule and reflect global properties such as contrast ratio and sparsity of dark channel. To capture global information and perform accurate dehazing, we introduced the Dehazformer block into our network because of the excellent dehazing abilities of the Dehazformer-Net [9]. Additionally, to reduce computational costs, the detailed parameters of the Dehazformer block in this paper are referred to the Dehazformer-Small in [9].

As exhibited in Fig. 2, the Transformer-based dehazing network is an enhanced 5-stage U-Net, which consists of three modules: a shallow feature extraction, a Mix DehazeFomer Block, and a reconstruction module.

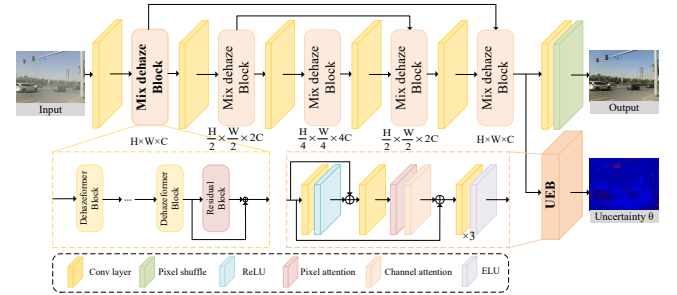


**Fig. 2.** Overview of our Transformer-based dehazing network.

**Shallow feature extraction.** A  $3 \times 3$  convolutional layer  $C_3(\cdot)$  is first applied to extract shallow feature information from the hazy image  $I \in \mathbb{R}^{H \times W \times 3}$ :

$$F_{\text{shallow}} = C_3(I) \quad (1)$$

**Mix DehazeFomer Block (MDB).** Next, feature  $F_{\text{shallow}}$  will be sent to Mix DehazeFomer Block for extracting image global features. In MDB, we first leverage several Dehazformer blocks  $DF(\cdot)$  (see Fig. 3) to extract the global information and then use the residual block without normalization layer  $RB(\cdot)$  to fuse the global information, such a hybrid structure is more efficient than using only Transformer

blocks. The global feature  $F_{global} \in R^{H \times W \times 3}$  is:

$$F_{global} = RB(DF(F_{shallow})_n) + DF(F_{shallow})_n \quad (2)$$

where  $n$  denotes the number of Dehazeformer blocks used in MDB.

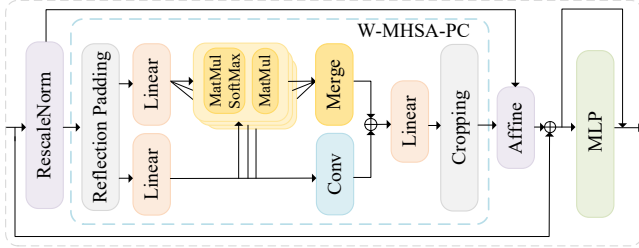


**Fig. 3.** Architecture of Dehazeformer block. W-MHSA-PC denotes the window-shifted multi-head self-attention with parallel convolution.

Reconstruction module. Finally, a  $3 \times 3$  convolutional layer  $C_3(\cdot)$  and a pixelshuffle layer  $P(\cdot)$  are used to produce the haze-free image  $J \in R^{H \times W \times 3}$  from the extracted  $F_{global}$ :

$$J = P(C_3(F_{global})) \quad (3)$$

### 2.3. Uncertain Estimated Block and Uncertain Loss

Theoretically, there are two types of uncertainty in Bayesian modeling: aleatoric uncertainty from the data and epistemic uncertainty from the model. The former is very common in dehazing models, but existing methods ignore exploring it. Therefore, we exploit an uncertainty estimation block (UEB) to predict the uncertainty of dehazing results, which enables the model to focus on regions with rich visual information (e.g., edge areas) to improve the final restoration results.

The prediction process for uncertainty  $\theta$  [14] can be expressed as:

$$\hat{J}_i = G_1(I_i) + \epsilon\theta_i \quad (4)$$

where  $\hat{J}_i$ ,  $G_1(I_i)$ ,  $\epsilon$  and  $\theta_i$  denote the ground-truth, coarse dehazed image, Laplace distribution, and aleatoric uncertainty from the synthetic dehazed image, respectively. For a more accurate prediction of  $\theta_i$ , we introduce Jeffrey's prior [16] into the uncertainty estimation process. For  $\hat{J}_i$ ,  $G_1(I_i)$ , the Laplace distribution-characterized log-likelihood function and uncertainty estimation loss  $L_{ue}$  can be expressed as:

$$\ln p(\hat{J}_i|I_i) = -\frac{\|\hat{J}_i - G_1(I_i)\|_1}{\theta_i} - 2 \ln \theta_i - \ln 2 \quad (5)$$

$$L_{ue} = \frac{1}{N} \sum_{i=1}^N \exp(-\ln \theta_i) \|\hat{J}_i - I_i\|_1 + 2 \ln \theta_i \quad (6)$$

We employ  $L_{ue}$  to estimate the  $\theta$  more accurately. Then, through the guidance of  $\theta$ , we apply the uncertainty-guided

loss  $L_{ugs}$  to push the network to concentrate more on the reconstruction error area with large uncertainty in the dehazed image, to obtain accurate and confident dehazed results. The formula is shown in (7). In addition, inspired by the identity loss [17], we incorporate the uncertainty-guided loss  $L_{ugu}$  into the unsupervised branch, as shown in (8).

$$L_{ugs} = \frac{1}{N} \sum_{i=1}^N (\ln \theta_i - \min(\ln \theta_i)) \|\hat{J}_i - G_2(I_i)\|_1 \quad (7)$$

$$L_{ugu} = \frac{1}{N} \sum_{j=1}^N (\ln \theta_j - \min(\ln \theta_j)) \|J_j - G_2(J_j)\|_1 \quad (8)$$

where  $G_2(\cdot)$ ,  $J_j$ ,  $\theta_j$  represents the student network, real-world images, and uncertainty from real-world dehazed images, respectively.

### 2.4. Loss Functions

**Teacher network.** The overall loss functions for the teacher network are formulated as:

$$L_t = L_{ts} + L_{tu} \quad (9)$$

where  $L_{ts}$ ,  $L_{tu}$  refers to the loss functions of the supervised and unsupervised branches, respectively.

$$L_{ts} = \lambda_1 * L_{ue} + \lambda_2 * L_a \quad (10)$$

$$L_{tu} = \lambda_3 * L_{ide} + \lambda_4 * L_{dc} + \lambda_5 * L_{tv} \quad (11)$$

where  $L_a$ ,  $L_{ide}$ ,  $L_{dc}$ ,  $L_{tv}$  represent adversarial loss, identity loss [17], total variation loss and dark channel loss [10].

**Student network.** The overall loss functions for the student network are formulated as:

$$L_t = L_{ss} + L_{su} \quad (12)$$

where  $L_{ss}$ ,  $L_{su}$  refers to the loss functions of the supervised and unsupervised branches, respectively.

$$L_{ss} = \lambda_1 * L_{ugs} + \lambda_2 * L_a \quad (13)$$

$$L_{su} = \lambda_3 * L_{ugu} + \lambda_4 * L_{dc} + \lambda_5 * L_{tv} + \lambda_6 * L_{kl} \quad (14)$$

where  $L_{kl}$  denotes the KL divergence loss.

KL loss: Since the intermediate structure of the network tends to extract high-dimensional haze-related features, we choose the 3-th MDB to supply the synthetic hazy image embedding  $V_{syn}$  and the real-world image embedding  $V_{real}$ . And by taking  $V_{syn}$  as the pseudo-label of  $V_{real}$ , these two haze distribution features are transformed into high-dimensional vectors to calculate  $L_{kl}$  [15], which can be expressed as:

$$L_{kl} = KL(Softmax(V_{real}), Softmax(V_{syn})) \quad (15)$$

by which to enhance the similarity of haze distribution features between synthetic and real-world images.

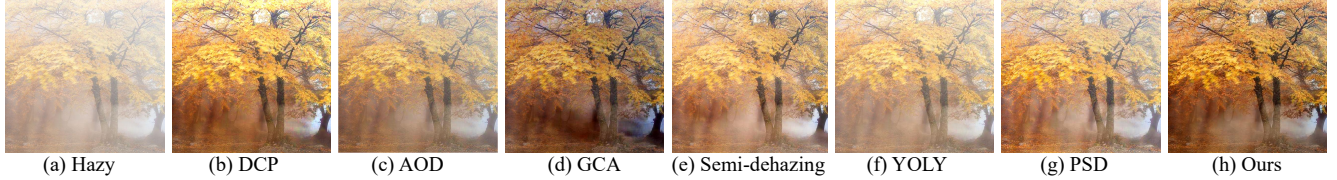


Fig. 4. Dehazing results on a real-world image.

### 3. EXPERIMENTS

#### 3.1. Implementation Details

Experiments are implemented on Pytorch 1.7 with NVIDIA RTX 3090 GPU and Adam optimizer with parameters  $\beta_1 = 0.9$ ,  $\beta_2 = 0.99$ ,  $\epsilon = 10^{-8}$  to train the network. The teacher network is trained for 100 epochs, in which we update the unsupervised branch once after updating the supervised five times. The student network is trained for 60 epochs, in which we update the supervised branch once after updating the unsupervised five times. In each stage, the learning rate is set to  $10^{-4}$  for the first half and then decays linearly to 0 at the end. The batch size is set to 2. The Semi-UFormer is trained with 10,000 paired and 2000 unpaired samples from the OTS and URHI datasets [18]. The loss weights are set to:  $\lambda_1 = 1$ ,  $\lambda_2 = 10^{-2}$ ,  $\lambda_3 = 2$ ,  $\lambda_4 = 10^{-2}$ ,  $\lambda_5 = 10^{-5}$ ,  $\lambda_6 = 10^{-6}$ .

#### 3.2. Comparison Results

Method	SOTS outdoor		HSTS		Time
	PSNR $\uparrow$	SSIM $\uparrow$	PSNR $\uparrow$	SSIM $\uparrow$	
DCP [3]	18.83	0.819	17.01	0.803	1.41
NCP [4]	18.07	0.802	17.62	0.798	1.45
AOD [5]	20.08	0.861	19.68	0.835	<b>0.11</b>
GCA [6]	21.66	0.867	21.37	0.874	0.21
EPDN [19]	22.57	0.863	20.37	0.877	0.23
GFN-IJCV [20]	24.21	0.849	23.17	0.829	0.43
Semi-dehazing [10]	24.79	0.892	24.36	0.889	0.32
YOLY [12]	20.39	0.889	21.02	0.905	40.56
PSD [11]	20.49	0.844	19.37	0.824	0.39
Ours	<b>26.87</b>	<b>0.928</b>	<b>28.72</b>	<b>0.934</b>	0.25

Table 1. Averaged PSNR, SSIM, and runtime (CPU/GPU) with state-of-the-art (SOTA) dehazing algorithms on synthetic datasets.

**Results on Synthetic Datasets.** Semi-UFormer is evaluated on the SOTS outdoor and HSTS sets [18] with nine SOTA dehazing algorithms. As exhibited in Table 1, our method achieves the highest PSNR and SSIM values on both datasets.

**Results on Real-world Images.** To evaluate the dehazing performance on real-world images, we apply the blind image quality evaluation index SSEQ [21], color evaluation index  $\sigma$  [22] and HCC [23]. Our Semi-UFormer produces the cleanest dehazed images with high visual quality compared with other dehazing approaches, as depicted in Fig. 4 and Table 2.

Method	SSEQ $\downarrow$	$\sigma\downarrow$	HCC $\uparrow$
DCP	38.402	0.0033	-0.1609
NCP	41.506	0.0154	-0.0220
GCA	38.400	0.0067	-0.0284
EPDN	38.632	<b>0.0009</b>	-0.0757
Semi-dehazing	<b>38.104</b>	0.0089	0.2124
PSD	40.912	0.0017	<b>0.6085</b>
Ours	<b>37.751</b>	<b>0.0001</b>	<b>0.2340</b>

Table 2. Quantitative comparisons (SSEQ/ $\sigma$ /HCC) with SOTA approaches on 50 real-world images. Red and blue colors are used to indicate the 1<sup>st</sup> and 2<sup>nd</sup> ranks, respectively.

Variants	Base	$V_1$	$V_2$	$V_3$
MDB	w/o	✓	✓	✓
Uncertainty	w/o	w/o	✓	✓
KL loss	w/o	w/o	w/o	✓
PSNR	24.74	25.34	26.17	<b>26.87</b>
SSIM	0.905	0.910	0.919	<b>0.928</b>

Table 3. Ablation Analysis on Semi-UFormer.

#### 3.3. Ablation Study

In ablation studies, we first build the base network with the original Dehazeformer-S module trained with  $L_1$  loss (replace the uncertainty loss). Then, we build base + MDB module  $\rightarrow V_1$ ,  $V_1$  + uncertainty  $\rightarrow V_2$ ,  $V_2$  + Knowledge Distillation  $\rightarrow V_3$  (full model). As exhibited in Table 3, our complete network scheme achieves the best dehazing performance.

## 4. CONCLUSION

In this work, a novel semi-supervised uncertainty-aware transformer network called Semi-UFormer is proposed for image dehazing, which leverages both real-world data and uncertainty guidance information to facilitate the dehazing tasks. To bridge the gap between synthetic and real data, we build our Semi-UFormer on top of a knowledge distillation framework and apply a two-branch network to train our model on both synthetic and real-world images. Moreover, we exploit an uncertainty estimation block (UEB) to predict the pixel uncertainty of the coarse dehazed results and then guide the network to better restore the image edges and structures. Experiments on both synthetic and real-world images fully validate the effectiveness of our Semi-UFormer.

## 5. REFERENCES

- [1] Yuhua Chen, Wen Li, Christos Sakaridis, Dengxin Dai, and Luc Van Gool, "Domain adaptive faster r-cnn for object detection in the wild," in *CVPR*, 2018, pp. 3339–3348.
- [2] Dong-Yoon Choi, Ji-Hoon Choi, Jinwook Choi, and Byung Cheol Song, "Sharpness enhancement and super-resolution of around-view monitor images," *IEEE TITS*, vol. 19, no. 8, pp. 2650–2662, 2017.
- [3] Kaiming He, Jian Sun, and Xiaoou Tang, "Single image haze removal using dark channel prior," *IEEE TPAMI*, vol. 33, no. 12, pp. 2341–2353, 2010.
- [4] Dana Berman, Shai Avidan, et al., "Non-local image dehazing," in *CVPR*, 2016, pp. 1674–1682.
- [5] Boyi Li, Xiulian Peng, Zhangyang Wang, Jizheng Xu, and Dan Feng, "Aod-net: All-in-one dehazing network," in *ICCV*, 2017, pp. 4770–4778.
- [6] Dongdong Chen, Mingming He, Qingnan Fan, Jing Liao, Liheng Zhang, Dongdong Hou, Lu Yuan, and Gang Hua, "Gated context aggregation network for image dehazing and deraining," in *WACV*, 2019, pp. 1375–1383.
- [7] Srinivasa G Narasimhan and Shree K Nayar, "Vision and the atmosphere," *IJCV*, vol. 48, no. 3, pp. 233–254, 2002.
- [8] Xu Qin, Zhilin Wang, Yuanchao Bai, Xiaodong Xie, and Huizhu Jia, "Ffa-net: Feature fusion attention network for single image dehazing," in *AAAI*, 2020, vol. 34, pp. 11908–11915.
- [9] Yuda Song, Zhuqing He, Hui Qian, and Xin Du, "Vision transformers for single image dehazing," *arXiv preprint arXiv:2204.03883*, 2022.
- [10] Lerenhan Li, Yunlong Dong, Wenqi Ren, Jinshan Pan, Changxin Gao, Nong Sang, and Ming-Hsuan Yang, "Semi-supervised image dehazing," *IEEE TIP*, vol. 29, pp. 2766–2779, 2019.
- [11] Zeyuan Chen, Yangchao Wang, Yang Yang, and Dong Liu, "Psd: Principled synthetic-to-real dehazing guided by physical priors," in *CVPR*, 2021, pp. 7180–7189.
- [12] Boyun Li, Yuanbiao Gou, Shuhang Gu, Jerry Zitao Liu, Joey Tianyi Zhou, and Xi Peng, "You only look yourself: Unsupervised and untrained single image dehazing neural network," *IJCV*, vol. 129, no. 5, pp. 1754–1767, 2021.
- [13] Yongzhen Wang, Xuefeng Yan, Donghai Guan, Mingqiang Wei, Yiping Chen, Xiao-Ping Zhang, and Jonathan Li, "Cycle-snsrgan: Towards real-world image dehazing via cycle spectral normalized soft likelihood estimation patch gan," *IEEE TITS*, 2022.
- [14] Qian Ning, Weisheng Dong, Xin Li, Jinjian Wu, and Guangming Shi, "Uncertainty-driven loss for single image super-resolution," *NeurIPS*, vol. 34, pp. 16398–16409, 2021.
- [15] Xin Cui, Cong Wang, Dongwei Ren, Yunjin Chen, and Pengfei Zhu, "Semi-supervised image deraining using knowledge distillation," *IEEE TCSVT*, 2022.
- [16] Mário Figueiredo, "Adaptive sparseness using jeffreys prior," *NeurIPS*, vol. 14, 2001.
- [17] Jun-Yan Zhu, Taesung Park, Phillip Isola, and Alexei A Efros, "Unpaired image-to-image translation using cycle-consistent adversarial networks," in *ICCV*, 2017, pp. 2223–2232.
- [18] Boyi Li, Wenqi Ren, Dengpan Fu, Dacheng Tao, Dan Feng, Wenjun Zeng, and Zhangyang Wang, "Benchmarking single-image dehazing and beyond," *IEEE TIP*, vol. 28, no. 1, pp. 492–505, 2019.
- [19] Yanyun Qu, Yizi Chen, Jingying Huang, and Yuan Xie, "Enhanced pix2pix dehazing network," in *CVPR*, 2019, pp. 8160–8168.
- [20] Xinyi Zhang, Hang Dong, Zhe Hu, Wei-Sheng Lai, Fei Wang, and Ming-Hsuan Yang, "Gated fusion network for degraded image super resolution," *IJCV*, vol. 128, no. 6, pp. 1699–1721, 2020.
- [21] Lixiong Liu, Bao Liu, Hua Huang, and Alan Conrad Bovik, "No-reference image quality assessment based on spatial and spectral entropies," *SPIC*, vol. 29, no. 8, pp. 856–863, 2014.
- [22] Zhengying Chen, Tingting Jiang, and Yonghong Tian, "Quality assessment for comparing image enhancement algorithms," in *CVPR*, 2014.
- [23] Yong Xu, Jie Wen, Lunke Fei, and Zheng Zhang, "Review of video and image defogging algorithms and related studies on image restoration and enhancement," *IEEE ACCESS*, vol. 4, pp. 165–188, 2015.